RSC Advances

PAPER

View Article Online
View Journal | View Issue

Cite this: *RSC Adv.*, 2017, **7**, 15077

Ag_2O/sodium alginate supramolecular hydrogel as a film photocatalyst for removal of organic dyes in wastewater

Yuhua Ma,[a] Jiajia Wang,[a] Shimei Xu,[b] Zhendong Zheng,[a] Juan Du,[a] Shun Feng*[ac] and Jide Wang*[a]

Received 20th December 2016
Accepted 28th February 2017

DOI: 10.1039/c6ra28468j

rsc.li/rsc-advances

A simple method was proposed to fabricate a Ag_2O supported alginate supramolecular hydrogel film using solution casting technology. The photocatalytic degradability of the film was investigated with methylene blue and malachite green as model dyes. Under irradiation of either UV or visible light, the photodegradation rates were above 93% for both dyes with relatively short degradation times. The film exhibited great adsorptivity of dyes (~76%), highly efficient charge separation and reusability (~90% of its initial activity after five runs). Furthermore, the potential photocatalytic mechanism was explored for the degradation of MB and MG with the film under visible light irradiation. This work provides a new insight into the fabrication of supramolecular hydrogel films as highly efficient photocatalysts for wastewater treatment in practice.

Introduction

The efficient removal of organic dyes from wastewater has been attracting a great deal of attention due to its ecological and environmental importance.[1–4] Over the past several decades, various techniques, *e.g.* adsorption, precipitation, coagulation and membrane separation, have been developed and applied to the treatment of organic dyes in wastewater.[5–7] But further handling, high power consumption and operating costs seriously limit their application in the manufacturing industry.[8,9] As a comparison, photocatalysis is highly efficient, more economic and greener.[10,11] Utilizing solar energy, organic dyes can be translated directly into environmentally safe products, water, carbon dioxide, mineral ions, *etc.*[9,12,13]

Nowadays, the most of reported photocatalysts are mainly in particle form. However, due to the inherent nature of the particle, it was difficult for post-separation and recycling, easy aggregation and corrosion.[9,14,15] Above defects can be solved in some degree by immobilizing catalysts on films. Moreover, they can provide fast charge carrier transport and can be regenerated and reused in a sustainable manner. Till now, a series of film-form photocatalysts were proposed through various approach, such as sputtering,[16] pulsed laser deposition,[17] spray pyrolysis deposition[18] and sol–gel method[19] on certain solid substrate. Among which, sol–gel method attracted much attention because of its distinct advantages including easier adjustment of composition and fabrication of large-area films, low cost and simple deposition equipment and so on.[20] However, the photocatalytic activity of the film would be negatively affected by the substrate through decrease the surface area and mobility.[14]

Recently, metal–polymer supramolecular hydrogel (SMH) has the unique 3D network structure as conventional hydrogel possessing, but the preparation was much more rapidly and economically.[21] SMH can be advised spontaneously with metallic cations as nodes and polymers through supramolecular complexation.[22] It has been successfully utilized in the fabrication of metal nanoparticles[23] and stimuli-responsive hydrogel.[22] Based on the steric structure of it, SMH should also be acted as a promising candidate for the photodegradation of dyes theoretically, if the metallic node was substituted with one atom or molecule with photocatalytic activity. But no reports on the feasibility of it as photocatalyst system were found.

Based on the point of view, one facile, environmentally friendly and cost-effective method was proposed to prepare one free-standing alginate SMH film immobilized with Ag_2O, one of the most promising photocatalysts for the degradation of dyes but seldom used as the principal photocatalytic material.[24,25] The morphology, structure and spectral information of it were characterized by multi-analytical tools. The photocatalytic activity of the as-prepared SMH film was investigated in aqueous solution with methylene blue (MB) and malachite green (MG) as model dyes under UV or visible light irradiation, respectively.

[a]*Key Laboratory of Oil & Gas Fine Chemicals, Ministry of Education, Xinjiang Uyghur Autonomous Region, College of Chemistry and Chemical Engineering, Xinjiang University, Urumqi, 830046, China. E-mail: fengshunxd@hotmail.com; awangjd@yahoo.com.cn*

[b]*College of Chemistry, Sichuan University, Chengdu 610064, China*

[c]*School of Life Science and Engineering, Southwest Jiaotong University, Chengdu 610031, China*

Experimental

Preparation of supramolecular hydrogel film

All chemicals were analytical grade and used without further purification. Solutions were prepared in de-ionized water. The formation procedure of Ag_2O/ALG SMH film was followed: in brief, a cuboid glass plate ($8.3 \times 8.4 \times 0.1$ cm^3) was casted by 7 mL of 2% (w/v) ALG solution. And then it was placed immediately into a glass culture dish containing 100 mL of 3% (w/v) $AgNO_3$ solution. Two seconds later, the SMH film was formed and further kept in $AgNO_3$ solution for 30 min. After that, the plate was taken out, and the film was removed out carefully. The resulted film was thoroughly rinsed with de-ionized water to remove any excess Ag^+ on the surface of the film. Finally, it was irradiated with a 250 W high pressure mercury lamp for 60 min. The film was stored in pure water before use.

Characterization

The dynamic rheological measurement was performed with a stress-controlled rheometer (Discovery HR-1, TA) using a 400 mm cone plate. Phase identification study of the hydrogel was carried out by XRD spectrum (XRD) using X-ray diffractometer (D8 Advance, Bruker) in 2θ range of 10–80° at a scan rate of 6° min^{-1} with Cu Kα radiation ($\lambda = 1.54178$ Å). The film's surface conditions and valence states in each component were characterized by an X-ray photoelectron spectroscopy (XPS, ESCALAB 250 Xi, Thermo Scientific) using monochromatized Al Kα excitation. All the binding energies were calibrated by referencing the C 1s peak at 284.6 eV. The morphology of the film was investigated using a field-emission scanning electron microscopy (FESEM, S-4800, Hitachi) and a transmission electron microscopy (TEM, JEM-2010F, JEOL). Surface area and pore size distribution of the film were measured by a JW-BK static nitrogen adsorption instrument (Beijing JWGB Sci. & Tech. Co., Ltd.). The static contact angle of oil on the film was measured at ambient temperature using a contact angle goniometer (JC2000C, Powereach Co.). UV-vis diffuse reflectance spectra (UV-vis DRS) were measured in the range of 200–1100 nm on a UV-vis diffuse reflectance spectrophotometer (4802S, Unico) equipped with an integral sphere using $BaSO_4$ as a reference. And photoluminescence spectra (PL) were measured using a fluorescence spectrophotometer (F-4500, Hitachi).

Photocatalytic experiments

Firstly, freshly prepared Ag_2O/ALG SMH film was immersed in 100 mL of MB or MG solution. And then, it was irradiated by a high pressure mercury lamp (365 nm, 250 W) or Xe lamp (>390 nm, 500 W) with an optical path of 20 cm. The concentration of dye in supernatant was monitored by a UV-vis spectrometer (Shimadzu UV-1780) at 665 nm to MB or 617 nm to MG at certain time intervals. The dye degradation rate (R) was then calculated based on the equation below:

$$R = \frac{(A_0 - A_t)}{A_0} \quad (1)$$

where R is the degradation rate, A_0 is the absorbance of the original solution, and A_t is the absorbance of the solution at any time.

Results and discussion

Formation of supramolecular hydrogel film

ALG is one kind of biopolymers, and owns both carboxylic and hydroxylic binding sites. Gelling and metal binding properties of it have been in the focus of research for many years. ALG can react with various metal cations (Ca^{2+}, Sr^{2+} or Ba^{2+}) and form SMH with the characteristic egg-box structure.[26] In this work, it was used to fabricate SMH with Ag^+. The hydrogelation procedure was straight-forward, requiring simply substituent of Na^+ of ALG with Ag^+, and Ag^+ would undergo the complexation with the ALG chains to form interwoven networks. It took only two seconds to finish the hydrogelation. Finally, the film was irradiated in water to translate Ag^+ into Ag_2O *in situ*.

Characterization of Ag_2O/ALG SMH film

The mechanical properties of Ag_2O/ALG SMH film were characterized by rheology at 25 °C. Firstly, the dynamic strain sweep was conducted within the strain region of 0.01–100% with a frequency of 1.0 rad s^{-1}, and the corresponding strain was determined to be 0.5%. Then a dynamic frequency sweep experiment was carried out in the region of 0.1–100 rad s^{-1} at the strain of 0.5%. As shown in Fig. 1, the storage modulus G' values of the film were greater than the loss modulus G'' values over the whole measurement period. It indicated that the hydrogel possessed a permanent network and was a supramolecular hydrogel.[27–30]

Fig. 2 was the XRD spectrum of the film. In which, the diffraction peaks at 27.82°, 32.28°, 38.03° and 46.29° were respectively assigned to the (1 1 0), (1 1 1), (2 0 0) and (2 1 1) diffraction planes of Ag_2O (JCPDS no. 41-1104). The result testified a certain amount of Ag_2O with high degree of crystallinity. XPS survey spectrum (Fig. 3a) revealed that the main elements of the film were C, Ag and O. The content of Ag_2O in the film was as high as 6.72%. In Fig. 3b, the Ag $3d_{3/2}$ and Ag $3d_{5/2}$ photoelectrons at 368.4 and 374.4 eV were highly

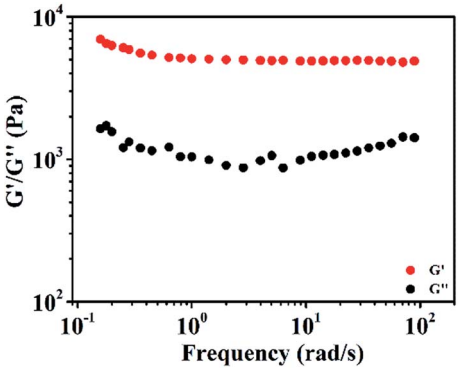

Fig. 1 Dynamic frequency sweep of the Ag_2O/ALG supramolecular hydrogel film at 0.5% strain.

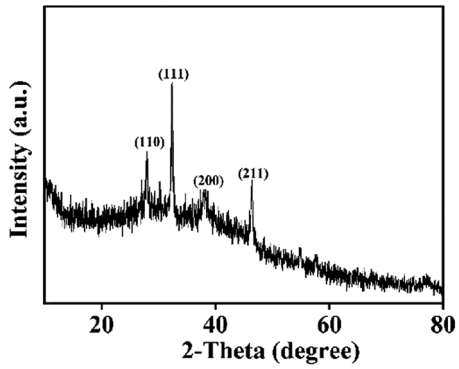

Fig. 2 XRD pattern of Ag_2O/ALG supramolecular hydrogel film.

consistent with values of Ag_2O.[31,32] And in Fig. 3c, the first component located at 531.3 eV was attributed to the oxygen of surface OH^- bound in the film, which would change into $^{\bullet}OH$ free radical during the photocatalytic reaction. It would be beneficial to photocatalysis process.[33] And the second component at 532.8 eV was corresponded to the oxygen in water molecules existed in the 3D network structure of the film.[34,35]

From FESEM images, it can be found that the film had a smooth surface with Ag_2O dispersed evenly and consistently (Fig. 4a), and an interconnected porous structure was obtained (Fig. 4c). Based on TEM images (Fig. 4b and d), the same result can be obtained. Also from Fig. 4d, it can be found that the size of Ag_2O was around 8.8 ± 1.0 nm. Such a small size can lead to a large photoactive area and high charge separation efficiency.[24,25,31]

The porous nature of the Ag_2O/ALG SMH film was determined by Brunauer–Emmett–Teller (BET) gas sorptometry measurements. The results were illustrated in Fig. 5. The isotherms were identified as type IV isotherms with type H3 hysteresis loop, the typical characteristic of mesoporous materials.[36] The pore-size distributions were in the range of 3 to

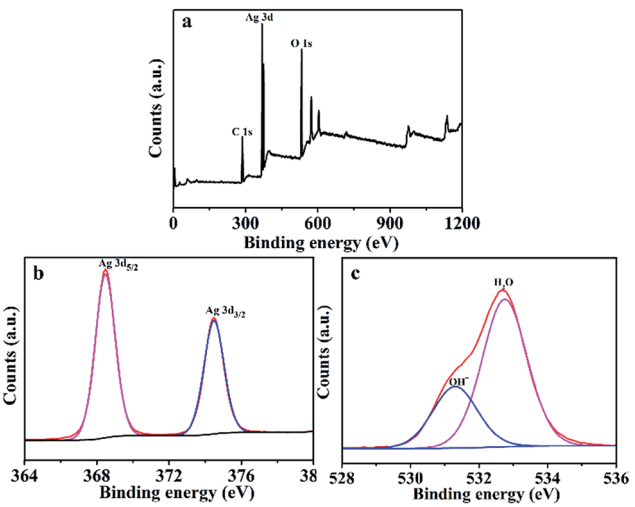

Fig. 3 (a) Survey XPS spectra of Ag_2O/ALG supramolecular hydrogel film. Deconvolution of XPS peaks of the Ag_2O/ALG supramolecular hydrogel film: (b) Ag 3d and (c) O 1s.

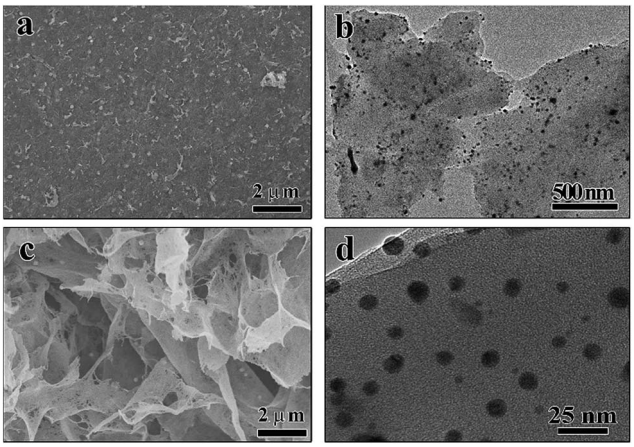

Fig. 4 FESEM image of Ag_2O/ALG supramolecular hydrogel film: (a) surface and (c) cross section; TEM spectra of Ag_2O/ALG supramolecular hydrogel film: (b) a typical and (d) an enlarged image.

30 nm, and the calculated BET specific surface area of the film was 24.48 $m^2\ g^{-1}$. The large mesoporous size distribution and high BET surface area were advantageous to adsorb more organic dyes on their surface, which will contribute to the enhancement of photocatalytic activity of catalysts.

The underwater oil wettability of the Ag_2O/ALG SMH film was evaluated. Firstly, the film was immersed in aqueous media, and then one droplet of oil (dichloroethane) was dipped in solution. As shown in Fig. 6, the oil droplet almost kept as a complete spherical with a contact angle to the film of 150.5° (larger than 150°), confirming the superoleophobicity of the film.[37] Above result demonstrated that the high possibility of using Ag_2O/ALG SMH film for the selective degradation of water-soluble organic dyes in aqueous systems.[38]

Photocatalytic property

To evaluate the photocatalytic activity of Ag_2O/ALG SMH film, degrading behaviors of organic dyes MB and MG were

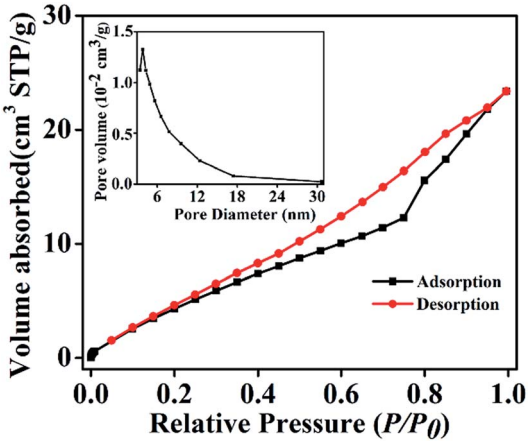

Fig. 5 Nitrogen adsorption–desorption isotherms and the corresponding pore size distribution curve (inset) of Ag_2O/ALG supramolecular hydrogel film.

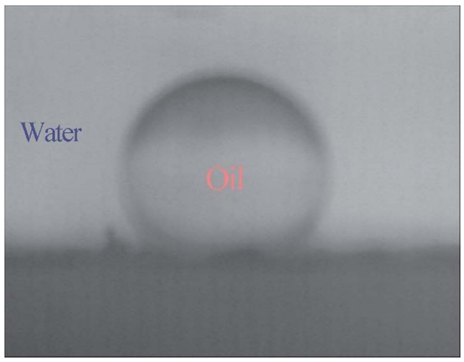

Fig. 6 Wetting behavior of Ag_2O/ALG supramolecular hydrogel film.

investigated. As shown in Fig. 7a, the degradation rate of MB was increased with the time gone and reached maximum of 95% in 150 min under visible irradiation or 93% in 180 min under UV irradiation. The rates were much higher than 76% obtained in dark for 180 min. To MG, the similar results were obtained, except that it took 270 min to reach the degradation equilibrium under either visible or UV irradiation (Fig. 7b). Compared with Ag-doped TiO_2 film (35%, under irradiation of UV light for 300 min)[39] and $TiO_2/SnO_2/CuInS_2$ film (92%, under irradiation of UV + visible light for 12 h),[40] Ag_2O/ALG SMH film showed the highest degradation rate and the shortest degradation time for the photodegradation of MB either under visible or UV irradiation. The excellent photodegradation performance was mainly attributed to the special 3D porous network the SMH film having, which made it absorb more solar irradiations and provided numerous approachable channels for charge transfer.[41,42] Furthermore, it is a free-standing film, which meant the active sites on both sides of film can be utilized.

It is well known that the adsorption capacity of the photocatalyst is one of the decisive factors affecting the photocatalytic activity of the catalyst. The high adsorption capacity of photocatalyst will facilitate the direct redox reactions of contaminant molecules.[43] From Fig. 7, it can be seen that over 76% MB or MG was adsorbed by the Ag_2O/ALG SMH film. The adsorption capacity of the film was calculated from the following equation:

$$q_e = \frac{(C_0 - C_e) \times V}{S} \quad (2)$$

where q_e is the adsorption capacity, C_0 is the initial concentration of the dye; C_e is the concentration of dye in solution at equilibrium time; V is the solution volume and S is the surface area of the film.

The calculated adsorption capacity of the film was 12.62 and 12.25 μg cm^{-2} to MB and MG, respectively. The high adsorption capacity to two dyes was attributed to the negatively charged ALG and the special 3D network structure (the large mesoporous size distribution and high BET surface area). It was a comprehensive result of various factors of electrostatic interaction and space.[44]

Furthermore, the pseudo-first-order and the pseudo-second-order modes were employed to describe the above degradation data as following:

$$\ln(q_e - q_t) = \ln q_e - k_1 t \quad (3)$$

$$\frac{t}{q_t} = \frac{1}{k_2 q_e^2} + \frac{t}{q_e} \quad (4)$$

where q_e and q_t represented the amount of dye degraded (μg cm^{-2}) at equilibrium and time t, respectively, and the k_1 and k_2 values were the kinetic rate constants. As shown in Table 1, the kinetic data can be accurately described by the pseudo-second-order model with a high correlation coefficient ($R^2 > 0.9896$).

Light absorption range

Fig. 8 illustrated UV-vis absorption spectrums of Ag_2O, ALG film and Ag_2O/ALG SMH film. Ag_2O clearly exhibited a wide and strong light absorption in the whole UV-vis range of 200–800 nm. While ALG film showed two weak absorption peaks in 210 and 304 nm. To Ag_2O/ALG SMH film, not only the photoresponding range was extended, but also the light absorption intensity was strengthened. Moreover, it can be estimated that the bandgap energy of Ag_2O/ALG SMH film was 1.24 eV narrower than that of Ag_2O (~1.3 eV) based on the intercept of the tangent to the plot. It demonstrated that the designed photocatalysts should have a better light response than Ag_2O since less energy was required to excite electrons from valence band to conduction band. Meanwhile light harvesting was improved through efficient light scattering due to the special 3D structure of Ag_2O/ALG SMH film.[12] And the extended light absorption range meant a broader spectral range of light (*e.g.* sunlight) can be utilized by the photocatalyst, therefore enhancing significantly the performance of photocatalysis.[45]

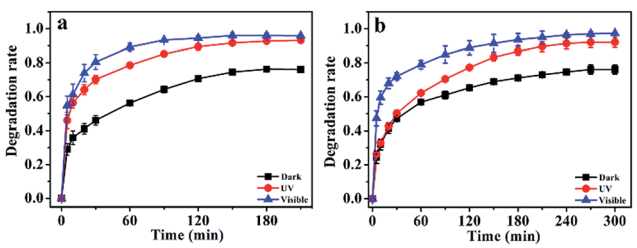

Fig. 7 Photocatalytic properties of Ag_2O/ALG supramolecular hydrogel film on (a) MB and (b) MG solutions at room temperature.

Table 1 Kinetic parameters of Ag_2O/ALG supramolecular hydrogel film on MB and MG degradations at room temperature

		Pseudo-first-order model		Pseudo-second-order model	
Dyes	Light	q_e (μg cm^{-2})	R^2	q_e (μg cm^{-2})	R^2
MB	Dark	8.789	0.9824	12.62	0.9896
	UV	8.527	0.9807	15.50	0.9981
	Visible	6.097	0.9779	15.11	0.9998
MG	Dark	7.957	0.9897	12.25	0.9955
	UV	12.33	0.9540	15.22	0.9921
	Visible	7.270	0.9816	15.70	0.9982

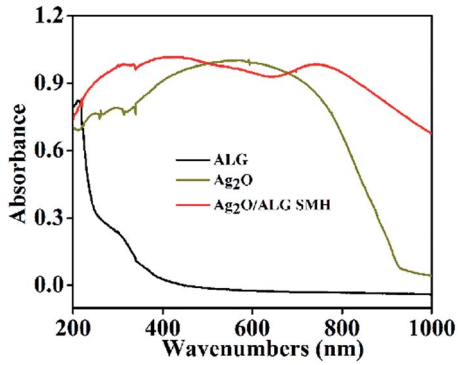

Fig. 8 UV-vis diffuse reflectance spectra of samples.

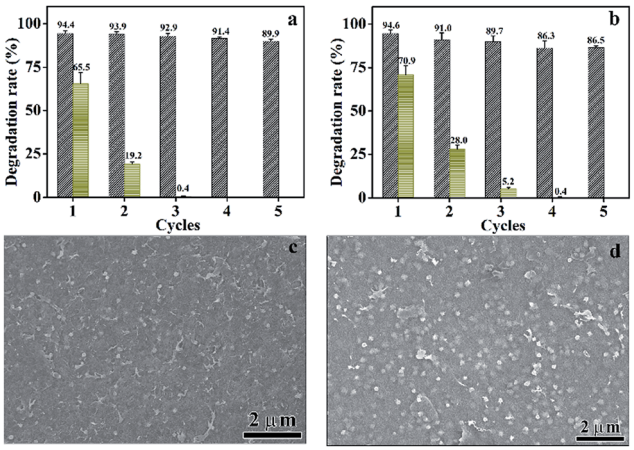

Fig. 10 Recycle and reuse of photocatalysts for (a) MB and (b) MG degradation under visible light irradiation; FESEM image of Ag_2O/ALG supramolecular hydrogel film: (c) fresh and (d) used after five successive reactions (oblique lines, Ag_2O/ALG supramolecular hydrogel film; straight line, Ag_2O).

Separation of photogenerated electron–hole pairs

Effective separation of the photogenerated electron–hole pairs is crucial for high-efficiency photocatalysts. In this work, PL was employed to investigate the interfacial charge-transfer process between Ag_2O and ALG in Ag_2O/ALG SMH film.[46] From Fig. 9, it can be found that the emission wavelength of the film was no distinct alteration after ALG introduced into film. However, fluorescence intensity of Ag_2O/ALG SMH film decreased, indicating that the film had a higher separation rate of photogenerated electrons and holes than Ag_2O having.

Reusability of Ag_2O/ALG SMH film

Theoretically, photogenerated holes in Ag_2O could transfer to the ALG (electron donors) before oxidizing the lattice O^{2-} and photogenerated electrons would be captured by O_2 before reducing lattice Ag^+. Above two processes would be helpful to maintain the structure of Ag_2O in Ag_2O/ALG SMH film under light irradiation.[47] To validate the assumption, it was used to photodegrade MB and MG successively. As shown in Fig. 10a and b, the catalytic activity of the Ag_2O/ALG SMH film can retain over 90% of its initial activity after five cycles. And it hardly to find difference between FESEM and XRD images of the film before and after five successive cycles of the reaction (Fig. 10c, d and 11). Above results testified the high stability the film had.

As comparison, Ag_2O almost lost its photodegradation activity in the third to MB and the fourth run to MG.[15,48,49] Here, the commercial ALG powders was also added directly into the solution of MB or MG. It was found that the concentration of MB or MG in the solution was decreased about 43.5% and 15.5% of its original concentration when ALG powders was used first time. When above pure ALG powders was used repeated, the concentration of dyes in solution was not change to either MB or MG with/without visible light irradiating. It demonstrated that the decrease of dye concentrations at pure ALG used in the first run was caused by the physical absorption of pure ALG powders, not the degradation of MB or MG. It indicated that pure ALG had no photocatalytic activity for the degradation of MB or MG.

Potential photocatalytic mechanism

The photocatalytic mechanism of degradation of MB and MG was explored. A set of free radical trapping experiments were performed by introducing scavenger of nitrogen

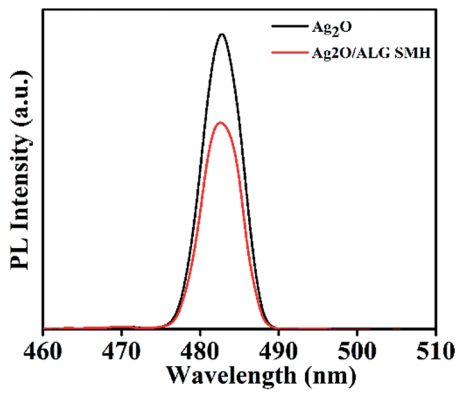

Fig. 9 Photoluminescence spectra of Ag_2O and Ag_2O/ALG supramolecular hydrogel film.

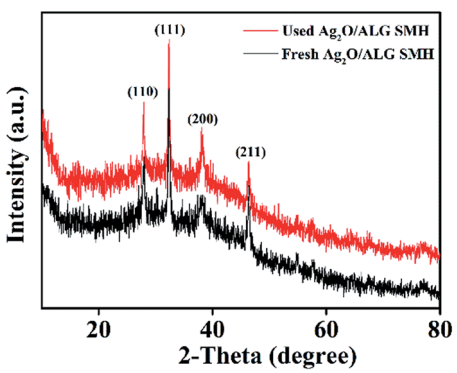

Fig. 11 XRD spectra of fresh and used Ag_2O/ALG supramolecular hydrogel film.

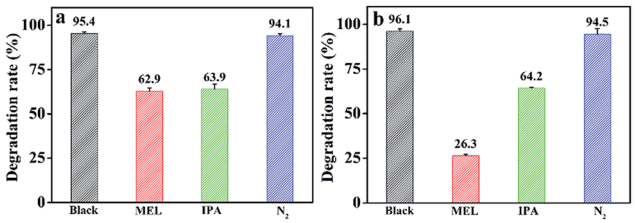

Fig. 12 The effect of different scavengers on the degradation of (a) MB and (b) MG in the presence of Ag_2O/ALG supramolecular hydrogel film (MEL: methanol; IPA: isopropanol).

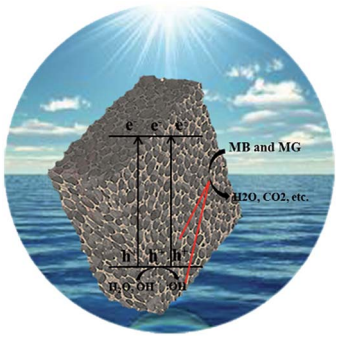

Fig. 13 The photocatalytic mechanism for the degradation of MB and MG with the Ag_2O/ALG supramolecular hydrogel film photocatalyst.

(N_2, $O_2^{\bullet-}$ quencher), 10 mL methanol (MEL, h^+ scavenger) or isopropylalcohol (IPA, $^{\bullet}OH$ radical scavenger) in the photocatalytic degradation process. As shown in Fig. 12a, the degradation rate slightly decreased by purging N_2 flow into the solution, indicating that few $O_2^{\bullet-}$ was involved in the degradation of MB. Notably, the photocatalytic degradation of MB decreased obviously with the addition of MEL or IPA. Therefore, it could be concluded that h^+ and $^{\bullet}OH$ were the main active species rather than $O_2^{\bullet-}$. The effects of above scavengers on the photodegradation rate of MG were almost as same to MB (Fig. 12b). The results demonstrated that h^+ and $^{\bullet}OH$ were the major reactive species of Ag_2O/ALG SMH film for the photodegradation of MB and MG.

Combined with above discussion and experiments, one possible mechanism for the photodegradation of MB and MG with Ag_2O/ALG SMH film was proposed and shown in Fig. 13. Firstly, the MB and MG were adsorbed by the film. Secondly, irradiated by the light, electrons were excited from valence band to conduction band, and were captured by O_2. At the same time, the abundant holes were left in valence band and transferred to ALG (electron donors).[47] The left h^+ would generate $^{\bullet}OH$ radicals. Finally h^+ and $^{\bullet}OH$ oxidized the MB and MG into H_2O, CO_2 and other inorganic salts.

Conclusions

In summary, Ag_2O/ALG SMH film photocatalyst was prepared by a solution casting technology. After that, Ag_2O were grown *in situ* onto the film by a convenient and "green" method. The film showed great adsorptivity of organic dyes, superoleophobicity, extended photoresponding range, and enhanced charge separation and transportation properties. It exhibited excellent photocatalytic degradability to organic dyes of MB and MG either under UV or visible light irradiation. Potential mechanism to photodegrade MB and MG was explored. It was found that h^+ and $^{\bullet}OH$ were the main active species contributing to the excellent photocatalytic degradation of the dyes. The film also showed high stability and reusability. We hope this finding could become a helpful template for people want to fabricate new type of photocatalyst.

Acknowledgements

This work was supported by the Doctor Student Research Innovation Project of Xinjiang (XJUBSCX-2014009), Natural Science Foundation of China (51541308) and NSFC-Xinjiang Joint Fund for Local Outstanding Youth (U1403392).

References

1 Z. Xiong and X. S. Zhao, *J. Am. Chem. Soc.*, 2012, **134**, 5754.
2 S. Wang, Y. Guan, L. Wang, W. Zhao, H. He, J. Xiao, S. Yang and C. Sun, *Appl. Catal., B*, 2015, **25**, 448.
3 C. Baslak, G. Arslan, M. Kus and Y. Cengeloglu, *RSC Adv.*, 2016, **6**, 18549.
4 W. Li, Y. Tian, P. Li, B. Zhang, H. Zhang, W. Geng and Q. Zhang, *RSC Adv.*, 2015, **5**, 48050.
5 C. Yang, U. Kaipa, Q. Z. Mather, X. Wang, V. Nesterov, A. F. Venero and M. A. Omary, *J. Am. Chem. Soc.*, 2011, **133**, 18094.
6 J. Dou, S. Yin, J. Y. Chong, B. Zhang, J. Han, Y. Huang and R. Xu, *Appl. Catal., A*, 2016, **513**, 106.
7 B. P. Nenavathu, A. V. R. Krishna Rao, A. Goyal, A. Kapoor and R. K. Dutta, *Appl. Catal., A*, 2013, **459**, 106.
8 J. Han, H. Y. Zeng, S. Xu, C. R. Chen and X. J. Liu, *Appl. Catal., A*, 2016, **527**, 72.
9 C. Wang, J. Li, X. Lv, Y. Zhang and G. Guo, *Energy Environ. Sci.*, 2014, **7**, 2831.
10 F. Lin, Y. Zhang, L. Wang, Y. Zhang, D. Wang, M. Yang, J. Yang, B. Zhang, Z. Jiang and C. Li, *Appl. Catal., B*, 2012, **127**, 363.
11 L. Dong, D. Liang and R. Gong, *Eur. J. Inorg. Chem.*, 2012, **2012**, 3200.
12 N. Wang, Y. Zhou, C. Chen, L. Cheng and H. Ding, *Catal. Commun.*, 2016, **73**, 74.
13 M. Zhang, W. Jiang, D. Liu, J. Wang, Y. Liu, Y. Zhu and Y. Zhu, *Appl. Catal., B*, 2016, **183**, 263.
14 D. Zhang, W. Wang, F. Peng, J. Kou, Y. Ni, C. Lu and Z. Xu, *Nanoscale*, 2014, **6**, 5516.
15 C. Yu, G. Li, S. Kumar, K. Yang and R. Jin, *Adv. Mater.*, 2014, **26**, 892.
16 S. Lee, E. Yamasue, H. Okumura and K. Ishihara, *Appl. Surf. Sci.*, 2015, **324**, 339.
17 R. Edla, N. Patel, M. Orlandi, N. Bazzanella, V. Bello, C. Maurizio, G. Mattei, P. Mazzoldi and A. Miotello, *Appl. Catal., B*, 2015, **166–167**, 475.

18 N. Hahn, S. Hoang, J. Self and C. Mullins, *ACS Nano*, 2012, **6**, 7712.
19 Y. Lim, C. Chua, C. Lee and D. Chi, *Phys. Chem. Chem. Phys.*, 2014, **16**, 25928.
20 Y. Li, L. Xu, X. Li, X. Shen and A. Wang, *Appl. Surf. Sci.*, 2010, **256**, 4543.
21 S. Bai, C. Sun, H. Yan, X. Sun, H. Zhang, L. Liang, X. Lei, P. Wan and X. Chen, *Small*, 2015, **11**, 5807.
22 Z. Sun, F. Lv, L. Cao, L. Liu, Y. Zhang and Z. Lu, *Angew. Chem., Int. Ed.*, 2015, **54**, 7944.
23 H. Yabu, K. Koike, K. Motoyoshi, T. Higuchi and M. Shimomura, *Macromol. Rapid Commun.*, 2010, **31**, 1267.
24 W. Zhou, H. Liu, J. Wang, D. Liu, G. Du and J. Cui, *ACS Appl. Mater. Interfaces*, 2010, **2**, 2385.
25 G. Wang, X. Ma, B. Huang, H. Cheng, Z. Wang, J. Zhan, X. Qin, X. Zhang and Y. Dai, *J. Mater. Chem.*, 2012, **22**, 21189.
26 O. Smidsrød and G. Skjåkbraek, *Trends Biotechnol.*, 1990, **8**, 71.
27 Y. Zhou, H. Cui, C. Shu, Y. Ling, R. Wang, H. Li, Y. Chen, T. Lu and W. Zhong, *Chem. Commun.*, 2015, **51**, 15294.
28 X. Li, G. Pu, X. Yu, S. Shi, J. Yu, W. Zhao, Z. Luo, Z. He and H. Chen, *RSC Adv.*, 2016, **6**, 62434.
29 H. Komatsu, S. Matsumoto, S. Tamaru, K. Kaneko, M. Ikeda and I. Hamachi, *J. Am. Chem. Soc.*, 2009, **131**, 5580.
30 S. Zu and B. Han, *J. Phys. Chem. C*, 2009, **113**, 13651.
31 M. Xu, L. Han and S. Dong, *ACS Appl. Mater. Interfaces*, 2013, **5**, 12533.
32 H. Yu, R. Liu, X. Wang, P. Wang and J. Yu, *Appl. Catal., B*, 2012, **111–112**, 326.
33 T. Sakamoto, T. Iida, T. Sekiguchi, Y. Taguchi, N. Hirayama, K. Nishio and Y. Takanashi, *J. Phys. D: Appl. Phys.*, 2008, **41**, 3080.
34 T. Jiao, H. Guo, Q. Zhang, Q. Peng, Y. Tang, X. Yan and B. Li, *Sci. Rep.*, 2015, **5**, 11873.
35 N. Salami, M. R. Bayati, F. Golestani-Fard and H. R. Zargar, *Mater. Res. Bull.*, 2012, **47**, 1080.
36 Y. Chen, G. Tian, G. Mao, R. Li, Y. Xiao and T. Han, *Appl. Surf. Sci.*, 2016, **378**, 231.
37 L. Zhang, Y. Zhong, D. Cha and W. Peng, *Sci. Rep.*, 2012, **3**, 670.
38 T. Wu, Q. Shao, S. Ge, L. Bao and Q. Liu, *RSC Adv.*, 2016, **6**, 58020.
39 A. Guillén-Santiago, S. Mayén, G. Torres-Delgado, R. Castanedo-Pérez, A. Maldonado and M. D. L. L. Olvera, *Mater. Sci. Eng., B*, 2010, **174**, 84.
40 A. Enesca, M. Baneto, D. Perniu, L. Isac, C. Bogatu and A. Duta, *Appl. Catal., B*, 2016, **186**, 69.
41 J. Cai, W. Liu and Z. Li, *Appl. Surf. Sci.*, 2015, **358**, 146.
42 H. Maleki, *Chem. Eng. J.*, 2016, **300**, 98.
43 W. Morales, M. Cason, O. Aina, N. R. de Tacconi and K. Rajeshwar, *J. Am. Chem. Soc.*, 2008, **130**, 6318.
44 J. Xu, L. Yang, X. Hu, S. Xu, J. Wang and S. Feng, *Soft Matter*, 2015, **11**, 1794.
45 Y. Lu, Y. Lin, D. Wang, L. Wang, T. Xie and T. Jiang, *Nano Res.*, 2011, **4**, 1144.
46 W. Zou, L. Zhang, L. Liu, X. Wang, J. Sun, S. Wu, Y. Deng, C. Tang, F. Gao and L. Dong, *Appl. Catal., B*, 2016, **181**, 495.
47 X. Wang, S. Li, H. Yu, J. Yu and S. Liu, *Chem.–Eur. J.*, 2011, **17**, 7777.
48 H. Wang, J. Li, P. Huo, Y. Yan and Q. Guan, *Appl. Surf. Sci.*, 2016, **366**, 1.
49 S. Yang, D. Xu, B. Chen, B. Luo and W. Shi, *Appl. Catal., B*, 2017, **204**, 602.